

# Reduced hind limb ischemia-reperfusion injury in Toll-like receptor-4 mutant mice is associated with decreased neutrophil extracellular traps

Rahmi Oklu, MD, PhD,<sup>a</sup> Hassan Albadawi, MD,<sup>b</sup> John E. Jones, MD,<sup>b</sup> Hyung-Jin Yoo, MS,<sup>b</sup> and Michael T. Watkins, MD,<sup>b</sup> *Boston, Mass*

**Objective:** Ischemia-reperfusion (IR) injury is a significant problem in the management of patients with acute limb ischemia. Despite rapid restoration of blood flow after technically successful open and endovascular revascularization, complications secondary to IR injury continue to occur and limit clinical success. Our aim was to create a murine model of hind limb IR injury to examine the role of Toll-like receptor-4 (TLR4) and to determine whether inactive TLR4 led to a decrease in the detection of neutrophil extracellular traps (NETs), which are known to be highly thrombogenic and may mediate microvascular injury.

**Methods:** A calibrated tension tourniquet was applied to unilateral hind limb of wild-type (WT) and TLR4 receptor mutant (TLR4m) mice for 1.5 hours to induce ischemia and then removed to initiate reperfusion. At the end of 48 hours of reperfusion, mice were euthanized and hind limb tissue and serum specimens were collected for analysis. Hematoxylin and eosin-stained sections of hind limb skeletal muscle tissue were examined for fiber injury. For immunohistochemistry, mouse monoclonal antihistone H2A/H2B/DNA complex antibody to detect NETs and rabbit polyclonal anti-myeloperoxidase antibody were used to identify infiltrating cells containing myeloperoxidase. Muscle adenosine triphosphate levels, nuclear factor (NF)- $\kappa$ B activity, the  $\alpha$ -subunit of inhibitor of NF- $\kappa$ B light polypeptide gene enhancer, poly (adenosine diphosphate-ribose) polymerase activity, and inducible nitric oxide synthase expression were measured. Systemic levels of keratinocyte-derived chemokine, monocyte chemoattractant protein-1, and vascular endothelial growth factor in the serum samples were also examined.

**Results:** IR injury in the hind limb of WT mice demonstrated significant levels of muscle fiber injury, decreased energy substrates, increased NF- $\kappa$ B activation, decreased levels of  $\alpha$ -subunit of inhibitor of NF- $\kappa$ B light polypeptide gene enhancer, increased inducible nitric oxide synthase expression, and increased poly (adenosine diphosphate-ribose) polymerase activity levels compared with the TLR4m samples. Additionally, there was marked decrease in the level of neutrophil and monocyte infiltration in the TLR4m mice, which corresponded to similar levels of decreased NET detection in the interstitial space and in microvascular thrombi. In situ nuclease treatment of WT tissue sections significantly diminished the level of NET immunostaining, demonstrating the specificity of the antibody to detect NETs and suggesting a potential role for nuclease treatment in IR injury.

**Conclusions:** These results suggest a pivotal role for TLR4 in mediating hind limb IR injury and suggest that NETs may contribute to muscle fiber injury. (*J Vasc Surg* 2013;58:1627-36.)

**Clinical Relevance:** Ischemia-reperfusion (IR) injury is a major problem in the treatment of peripheral vascular disease. To better understand its mechanism, a murine model of hind limb IR injury was created in Toll-like receptor-4 mutant mice. Results showed that mutant mice demonstrated significantly less IR-related injury compared with the wild-type mice. In addition, there was marked decrease in the level of neutrophil extracellular trap detection in the interstitial tissue and in vessels of the hind limb. These results indicate that Toll-like receptor-4 is a key player in murine hind limb IR injury and that systemic nuclease treatment may potentially ameliorate IR injury.

From the Divisions of Vascular Imaging and Intervention<sup>a</sup> and Vascular and Endovascular Surgery,<sup>b</sup> Harvard Medical School, Massachusetts General Hospital.

M.T.W. is the Isenberg Scholar in Academic Surgery at the Massachusetts General Hospital. This study was supported by National Institutes of Health Grant RO1-AR-055843 (M.T.W.), the Pacific Vascular Research Foundation, and the Department of Surgery, Division of Vascular and Endovascular Surgery (The Rosenberg Fund). R.O. is funded by the American College of Phlebology and the Department of Radiology, Division of Vascular Imaging and Intervention.

Author conflict of interest: none.

Reprint requests: Michael T. Watkins, MD, Massachusetts General Hospital, Division of Vascular and Endovascular Surgery, 15 Parkman St, Ste 440, Boston, MA 02114 (e-mail: mtwatkins@partners.org).

The editors and reviewers of this article have no relevant financial relationships to disclose per the JVS policy that requires reviewers to decline review of any manuscript for which they may have a conflict of interest.

0741-5214/\$36.00

Copyright © 2013 by the Society for Vascular Surgery.

<http://dx.doi.org/10.1016/j.jvs.2013.02.241>

The cornerstone for the treatment of acute limb ischemia is to rapidly restore blood flow to the limb to minimize ischemia-reperfusion (IR) injury, which occurs when blood is reintroduced into the oxygen-deprived limb. The mechanism of reperfusion injury is complex, involving a vigorous inflammatory response to reflow in which the innate immune system plays a central role. IR injury is in part mediated by proinflammatory cytokines, endothelial cell activation, reactive oxygen species, and neutrophil infiltration and activation. There is growing evidence linking the Toll-like receptor (TLR) family of proteins of the innate immune system, specifically TLR4, and the development of IR injury in myocardial infarction, stroke, intestinal ischemia, transplantation, and sepsis.<sup>1-4</sup> The role of TLR4 in IR has been largely derived from murine models deficient in the functional form of the TLR4 gene. Deficiency of TLR4 provides significant protection from tissue injury in hepatic transplant models and in murine models of cardiac, cerebral, and renal IR and hemorrhagic shock.<sup>1,4-7</sup>

Neutrophils play a key role in the inflammatory response raised against IR injury. The accumulation of neutrophils into an inflamed site is directed by cytokines and, upon activation, neutrophils can release neutrophil extracellular traps (NETs), which consist of neutrophil genomic DNA studded with cytoplasmic granular proteins released into the extracellular matrix.<sup>8</sup> Although NETs were initially detected in infectious tissues, such as in appendicitis, shigellosis, fasciitis, and pneumonia, they have also been detected in plasma and thrombus.<sup>9-11</sup> In infection, NETs seem to have a protective, antimicrobial effect. In thrombosis, however, NETs appear to have a deleterious effect by playing a role in clot formation directly by stimulating platelets via the TLR4 pathway.<sup>3,9,12,13</sup>

This study designed experiments to test the hypothesis that TLR4 modulates skeletal muscle injury, inflammation, and the production of NETs in response to IR. To test this hypothesis, murine hind limb IR injury was created in wild-type (WT) and TLR4 mutant (TLR4m) mice. Several factors were examined to assess structural muscle damage (histologic examination), skeletal muscle energy metabolism (adenosine triphosphate [ATP]), and markers of inflammation (inducible nitric oxide synthase [iNOS] messenger RNA [mRNA], poly [adenosine diphosphate (ADP)-ribose] polymerase [PARP] activity), expression of p65 nuclear factor (NF)- $\kappa$ B protein, and the  $\alpha$ -subunit of the inhibitor of NF- $\kappa$ B protein (I- $\kappa$ B $\alpha$ ), systemic inflammation (serum cytokines), and angiogenesis (serum vascular endothelial growth factor [VEGF]). Lastly, the detection of NETs within the injured hind limb was examined using immunohistochemistry to determine whether the functional status of TLR4 was associated with the amount of NETs detected and the level of tissue injury.

## METHODS

Animal care and experimental procedures were in compliance with the "Principals of Laboratory Animal

Care" (*Guide for the Care and Use of Laboratory Animals*, U.S. National Institutes of Health publication No. 85-23, National Academy Press, Washington, D.C., revised 1996) and approved by the Institutional Review Committee.

**Animal protocols.** C3H/HeJ TLR4m<sup>14</sup> and WT C3H/HeSnJ mice (8 to 12 weeks old; The Jackson Laboratory, Bar Harbor, Me) were housed in pathogen-free cages and given free access to water and standard rodent chow. As previously described, 1.5 hours of hind limb ischemia, followed by reperfusion, was created.<sup>15</sup> After 48 hours of reperfusion, mice were euthanized and hind limb tissue and serum specimens were collected. Hind limbs were fixed for histologic analysis or immediately frozen in liquid nitrogen and stored at  $-80^{\circ}\text{C}$  for future analysis.

## HISTOLOGY AND IMMUNOHISTOCHEMISTRY

**Muscle injury.** Transverse 5- $\mu\text{m}$  sections of hind limb muscle tissue were stained with hematoxylin and eosin (H&E) to visualize tissue morphology. To determine muscle fiber injury in each of the hind limb specimens (WT, n = 8; TLR4m, n = 8), 16 images from the H&E stained sections (original magnification,  $\times 200$ ) of the anterior tibialis and gastrocnemius muscle groups were obtained using a light microscope after 48 hours of reperfusion. Each image was assigned a distinct number using SPOT Insight microscope camera software (Diagnostic Instruments, Sterling Heights, Mich) and analyzed as previously described.<sup>16</sup> Muscle fiber injury was indicated by the presence of destroyed cell membrane, loss of nuclear morphology, and loss of polygonal shape of the muscle fiber. The data were expressed as the percentage of injured fibers from the total number of muscle fibers counted in each tissue sample, as previously described.<sup>16</sup>

**Inflammatory cell infiltration.** Because myeloperoxidase (MPO) is produced by neutrophils and macrophages,<sup>17,18</sup> tissue sections were immunostained for this protein (WT, n = 8; TLR4m, n = 8). Rabbit polyclonal anti-MPO (Abcam, Cambridge, Mass) was used for detection at a concentration of 1  $\mu\text{g}/\text{mL}$ . The secondary antibody, antirabbit immunoglobulin G (IgG) conjugated to horseradish peroxidase enzyme (Vector Labs, Burlingame, Calif), was also used in the same concentration. Sections were developed using 3,3'-diaminobenzidine chromogen reagent solution (R&D Systems, Minneapolis, Minn) according to the manufacturer's instructions. A Carl Zeiss microscope (100TV; Carl Zeiss Microimaging, Thornwood, NY) with a multiband filter block was used to visualize the tissue sections. Images of these sections were taken using a Quantifire X1 digital camera (Optronics, Goleta, Calif) and processed using Pictureframe software (Optronics). For negative controls, the MPO antibody was substituted with 1  $\mu\text{g}/\text{mL}$  dilution of the antirabbit IgG.

Similar to the quantitation of the muscle fiber assay, 20 images at original magnification  $\times 200$  for each hind limb muscle tissue section immunostained for MPO were assigned a number using a random number generator. Sixteen of the 20 images from each hind limb tissue

were uploaded using Photoshop software (Adobe, San Jose, Calif), and a blinded reviewer counted all MPO-positive cells. The data are expressed as mean number of MPO-positive cells/high-power field (HPF; original magnification  $\times 200$ )  $\pm$  standard error for each group.

**NET detection.** Hind limb tissue sections (WT,  $n = 8$ ; TLR4m,  $n = 8$ ) were developed using a cyanine-3 tyramide signal amplification kit (PerkinElmer Life, Boston, Mass) according to the manufacturer's instructions. The mouse monoclonal antihistone H2A/H2B/DNA complex antibody (gift of Dr Marc Monestier, Temple University, Pa) and the antimouse IgG antibody (Vector Labs) were used to detect NETs at 1  $\mu\text{g}/\text{mL}$  dilution.<sup>19</sup> Sections for immunofluorescence were mounted using Vectashield mounting medium (Vector Labs) containing 4',6'-diamidino-2-phenylindole. As above, a Carl Zeiss microscope (100TV) was used to image the immunofluorescent slides. For negative control, the NET antibody was omitted and substituted with 1  $\mu\text{g}/\text{mL}$  dilution of the antimouse IgG. To demonstrate the specificity of the mouse monoclonal antihistone H2A/H2B/DNA complex antibody to detect NETs, a subset of tissue sections were initially treated with 10 units of DNase enzyme (New England BioLabs, Ipswich, Mass) for 30 minutes at 37°C. These sections were not treated with Triton X-100 to minimize permeabilization.

**Muscle ATP quantitation.** Two hundred milligrams of each frozen hind limb muscle tissue (WT,  $n = 5$ ; TLR4m,  $n = 5$ ) was homogenized on ice in 10% trichloroacetic acid using a polytron tissue disruptor. The supernatant from each sample was collected after centrifugation for 10 minutes at 10,000*g* at 4°C. Each sample was diluted using Dulbecco's modified phosphate-buffered saline (with  $\text{Ca}^{2+}$  and  $\text{Mg}^{2+}$ , pH, 7.4). ATP levels (nmol/mg tissue) were measured using the ATPlite luminescence assay (PerkinElmer Life), following the manufacturer's instructions.

**NF- $\kappa$ B activity.** Total nuclear protein extracts were prepared from fresh hind limb tissue (WT,  $n = 5$ ; TLR4m,  $n = 5$ ) using a nuclear extraction kit (Active Motif, Carlsbad, Calif), following the manufacturer's instructions. Briefly, tissue (200 mg) was trimmed from the posterior calf muscle, rinsed in ice cold phosphate-buffered saline, and immediately homogenized in a hypotonic buffer supplemented with 1  $\mu\text{L}$  of a detergent mix and 1  $\mu\text{L}/\text{mL}$  of 1M dithiothreitol. The homogenate was placed on ice for 30 minutes and centrifuged for 10 minutes at 850*g* at 4°C. The pellet was resuspended in a hypotonic buffer, and 50  $\mu\text{L}/\text{mL}$  of detergent was added for each milliliter of total volume and then mixed and centrifuged for 30 seconds at 14,000*g*. The supernatant was decanted and the pellet resuspended in a lysis buffer. Samples were rocked on ice for 30 minutes and centrifuged for 10 minutes at 14,000*g* at 4°C. The supernatant was collected, and aliquots were stored at  $-80^\circ\text{C}$  until analysis.

The concentration of the proteins was determined using a bicinchoninic acid assay with bovine serum albumin as the standard (Pierce Biotechnology, Rockford, Ill),

following the manufacturer's instructions. To estimate NF- $\kappa$ B activation in the hind limb tissues, a Trans-AM NF- $\kappa$ B p65 Transcription Factor Assay Kit (Active Motif, Carlsbad, Calif) was used, following the manufacturer's instructions. The assay used 20  $\mu\text{g}$  of each of the nuclear protein samples. Results are presented as a mean optical density 450 nm  $\pm$  standard error of the mean.

**I $\kappa$ B $\alpha$  expression and PARP activity.** One hundred micrograms of total protein isolated from each hind limb tissue (WT,  $n = 5$ ; TLR4m,  $n = 5$ ) was solubilized with equal volume of Laemmli sample buffer (0.25M Tris-HCl [pH 6.8], 8% sodium dodecyl sulfate, 40% glycerol, 0.4M dithiothreitol, and 0.04% Bromophenol Blue; BioRad, Hercules, Calif), boiled for 5 minutes, and then loaded onto lanes at 4% to 15% density gradient on Tris-HCl sodium dodecyl sulfate-polyacrylamide gel. Samples were subjected to electrophoresis, followed by electroblotting transfer using a 0.22- $\mu\text{m}$  nitrocellulose membrane (BioRad). The membranes were blocked with Western blot blocker (Sigma-Aldrich, St. Louis, Mo) for 1 hour at room temperature. To assess PARP activity, the membranes were incubated with monoclonal anti-PARP antibody (1:2000 dilution, Tulip Biolabs, West Point, Pa) that detects PARP-modified proteins in the muscle extracts.

To determine the level of total and phosphorylated I $\kappa$ B $\alpha$ , membranes were incubated with polyclonal rabbit anti-I $\kappa$ B $\alpha$  antibody or polyclonal rabbit antiphospho-I $\kappa$ B $\alpha$  (pSer32) antibody (1:1000 dilution for both antibodies; Cell Signaling Technology, Danvers, Mass) for 1 hour at room temperature. Membranes were probed with goat antimouse or goat antirabbit horseradish peroxidase-conjugated IgG (1:4000 dilution) in blocking buffer for 1 hour at room temperature. The membranes were washed and developed using the enhanced chemiluminescence detection system (GE Healthcare, Piscataway, NJ). The generated specific protein band integrated density values (IDVs) were measured using the FluorChem HD2 Imager system (Cell Biosciences, Santa Clara, Calif). The membranes were stripped and reprobed using antimouse  $\alpha$ -tubulin IgG (Abcam).

#### iNOS mRNA expression

**Semi-quantitative reverse transcription-polymerase chain reaction.** Total RNA was isolated from hind-limb tissue (WT,  $n = 5$ ; TLR4m,  $n = 5$ ) after homogenization in Trizol Reagent (Invitrogen, Carlsbad, Calif), followed by chloroform phase separation and 2-propanol precipitation. Total RNA samples were purified by silica gel membrane column (Qiagen, Valencia, Calif). The concentration of total RNA was determined by measuring the absorption at 260 nm, and the purity of the purified RNA was assessed by the ratio between the absorbance values at 260 and 280 nm. Equal amounts of total RNA were reverse-transcribed using the SuperScript First-Strand Synthesis System (Invitrogen) and Oligo (dT) primers. iNOS complementary DNA was amplified using platinum blue polymerase chain reaction super mix as follows: 94°C for 30 seconds, 55°C for 30 seconds, and 72°C for 60

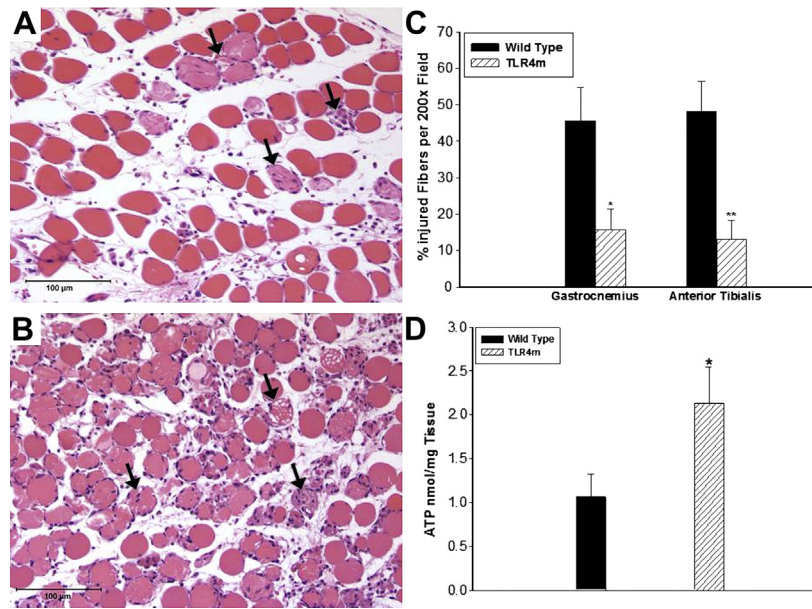


**Fig 1.** Representative images are shown of hematoxylin and eosin staining of the murine hind limb muscle tissue sections after 1.5 hours of ischemia and 48 hours of reperfusion. **A**, Tissue sections from Toll-like receptor-4 mutant (*TLR4m*) mice show relatively preserved muscle fibers with scattered fiber injury (*black arrows*) and tissue edema (*black bar* = 100  $\mu$ m). **B**, Wild-type (WT) tissue sections show significantly greater muscle fiber injury, with *black arrows* indicating examples of injured fibers (*black bar* = 100  $\mu$ m). **C**, There was significantly greater muscle fiber injury in the WT hind limb muscle groups, gastrocnemius, and anterior tibialis, compared with the TLR4m tissues (\* $P < .05$ , \*\* $P < .01$ , respectively). **D**, Increased muscle fiber injury in WT mice was consistent with significantly decreased adenosine triphosphate (ATP) levels compared with the less injured TLR4m group showing much higher ATP levels (\* $P < .04$ ).

seconds for a total of 30 cycles. Primer pair sequences used for iNOS were previously described.<sup>20</sup> The following  $\beta$ -actin primers were used:

5'-CAGGTCATCACTATTGGCAACG-3' and 5'-CACAGAGTACTTGGCTCAGGA-3' for 26 cycles. The reaction mix of each sample was subjected to 1.5% agarose electrophoreses in TAE (Tris base, acetic acid, and ethylenediaminetetraacetic acid) buffer. Alpha Imager 1000 system (Alpha Innotech Corp, San Leandro, Calif) was used to calculate the bands IDVs after background correction. Data were normalized to  $\beta$ -actin band densities.

**Serum cytokines and VEGF.** Serum aliquots (WT,  $n = 8$ ; TLR4m,  $n = 8$ ) obtained after 48 hours of reperfusion were assayed for keratinocyte-derived cytokine (KC), monocyte chemoattractant protein-1 (MCP-1), and vascular endothelial growth factor (VEGF) using quantitative enzyme-linked immunosorbent assay (R&D Systems), according to the manufacturer's protocol.

**Statistical analysis.** Statistical analysis between two groups was performed with InStat software (GraphPad, San Diego, Calif) using parametric and nonparametric unpaired  $t$ -tests. The results are expressed as the mean  $\pm$  standard error.

## RESULTS

**Muscle fiber injury.** Muscle fiber injury in the WT group was significantly greater than in the TLR4m samples

(WT,  $45.5 \pm 9\%$  vs TLR4m,  $15.8 \pm 6\%$  injured fibers;  $n = 8/\text{group}$ ;  $P < .03$ ; Fig 1, C) indicating that inactive TLR4 receptor signaling preserves muscle fiber integrity during IR. Representative photomicrographs of the reperfused skeletal muscle in TLR4m and WT are demonstrated in Fig 1, A and B, respectively. There were no differences in skeletal muscle morphology between non-ischemic sham-operated WT and TLR4m mice (data not shown).

**MPO immunostaining of reperfused skeletal muscle.** Quantitative analysis of MPO immunostaining of reperfused skeletal muscle from WT and TLR4m mice showed significantly more MPO-positive cells in the WT mice ( $245 \pm 28$  cells/HPF) than in the TLR4m mice ( $53 \pm 17$  cells/HPF;  $n = 8/\text{group}$ ;  $P < .0001$ ; Fig 2). These infiltrates were more prominent in the interstitial and perivascular regions of WT (Fig 2, B) than in the TLR4m mice (Fig 2, A). The tissue sections of the contralateral hind limbs not subjected to IR showed no evidence of MPO-positive immunostaining.

**Expression of NETs in reperfused skeletal muscle.** Regions demonstrating increased cell density that were positive for the MPO marker also revealed intense immunostaining for NETs (Fig 3). More NETs were detected in the WT group (Fig 3, A) than in the TLR4m group (Fig 3, B), mirroring the level of neutrophil detection by MPO (Fig 2). NETs were found largely in the



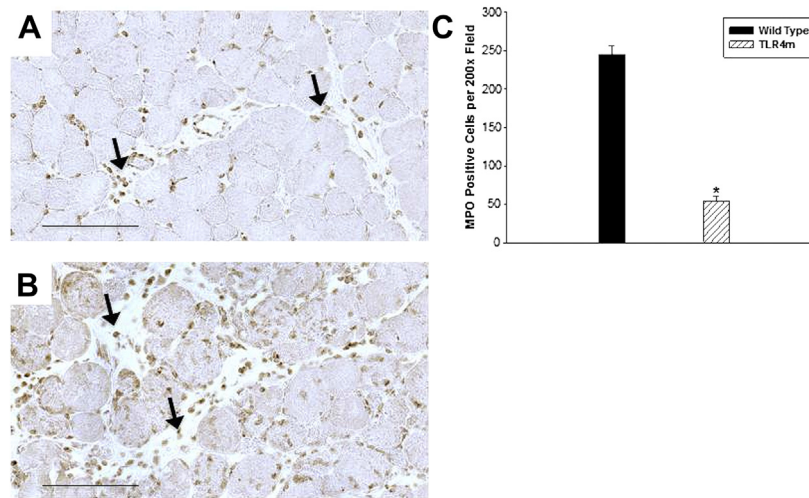


**Fig 2.** **A**, Representative images are shown of immunohistochemical detection of myeloperoxidase (MPO) in murine hind limb muscle tissue sections after 1.5 hours of ischemia and 48 hours of reperfusion (*black bar* = 100  $\mu$ m). **B**, Immunostaining of specimens from Toll-like receptor-4 mutant (*TLR4m*) mice showed significantly less MPO-positive cells (*brown*) in muscle tissue than the wild-type (WT) group. The *black arrows* indicate examples of MPO-positive cells (*black bar* = 100  $\mu$ m). **C**, There were more than fivefold greater MPO immunostained cells within the tissue sections of WT mice compared with the *TLR4m* mice (\**P* < .0001).

interstitial tissue, perivascular space, and within microvascular thrombi. The amount of NET immunostaining was significantly lower in sections from the *TLR4m* mice and was undetectable tissue sections from the control contralateral hind limb (Fig 3, C), providing evidence that the origin of these NETs is predominantly the neutrophils.

To explore the possibility of using DNase as a potential therapeutic agent to degrade the NETs and to demonstrate the specificity of the antibody to detect NETs, WT tissue sections were immunostained for NETs after DNase treatment. The immunofluorescent images revealed a marked decrease in the detection of NETs in the interstitial, perivascular, and microvascular thrombi of the WT sections after DNase treatment (Fig 4).

#### Biochemical characterization of reperfused skeletal muscle

**Expression of iNOS mRNA.** *TLR4m* mice had significantly less iNOS expression than WT mice at 48 hours (*n* = 5/group; *P* < .03; Fig 5). This finding suggests that *TLR4* modulates expression of iNOS in skeletal muscle during hind limb IR injury.

**Adenosine triphosphate.** *TLR4m* samples contained significantly higher levels of ATP than WT samples after IR (*TLR4m*:  $2.1 \pm 0.4$  vs WT:  $1.06 \pm 0.3$  nmol/mg tissue; *n* = 5/group; *P* = .04; Fig 1, D). This finding further suggests that in the absence of functional *TLR4*, there are preserved levels of ATP consistent with decreased levels of muscle fiber injury, as demonstrated by histology.

**NF- $\kappa$ B activity and I $\kappa$ B $\alpha$  expression.** To estimate the level of NF- $\kappa$ B activation in the hind limb tissues of the WT and the *TLR4m* groups, nuclear extracts were assayed, revealing significant differences after 1 hour of

reperfusion. The relative activation of the p65 subunit of NF- $\kappa$ B in the *TLR4m* group was significantly less than the WT mice (*TLR4m*,  $0.7342 \pm 0.05$  vs  $1.145 \pm 0.11$  AU; *n* = 5/group; *P* < .01; Fig 6, A). Thus, the acute activation of the transcription factor NF- $\kappa$ B was markedly decreased in the *TLR4m* group compared with the WT mice. At 48 hours of reperfusion, however, p65 NF- $\kappa$ B activity was not significantly different between the two groups (*TLR4m*,  $0.59 \pm 0.1$  vs  $0.53 \pm 0.09$  AU; *P* < .69; Fig 6, A), suggesting that there may be an overlap between other cell receptor signaling pathways.

To further support the idea that the initial NF- $\kappa$ B activation is markedly decreased in *TLR4m* mice, Western blotting analysis showed that the expression of the total I $\kappa$ B $\alpha$  subunit protein was significantly elevated in the hind limb muscle tissue of the *TLR4m* mice compared with the WT mice at 1 hour of reperfusion (*TLR4m*:  $28761 \pm 2282$  vs WT:  $16934 \pm 1493$  IDV; *P* < .003; Fig 6, B and C). The quantity of phosphorylated I $\kappa$ B $\alpha$  protein, however, was not significantly different between the two groups (*TLR4m*:  $9456 \pm 1987$ , WT:  $4992 \pm 3382$  IDV; *P* < .06; Fig 6, B and C).

**PARP activity.** *TLR4m* mice showed a significant decrease in the PARP-modified proteins at 48 hours' reperfusion compared with WT ( $3.86 \pm 0.87$  for *TLR4* vs  $8.1 \pm 1.6$  IDV ratio; *n* = 5/group; *P* = .03; Fig 6, D and E). These data suggest that modification of PARP has been reduced in *TLR4m*, which implicates a link between PARP activity and *TLR4* signaling pathway activity during skeletal muscle reperfusion injury.

**Systemic markers of inflammation.** CXC/KC (neutrophil chemokine), MCP-1, and VEGF levels in the serum samples of WT were compared with *TLR4m*

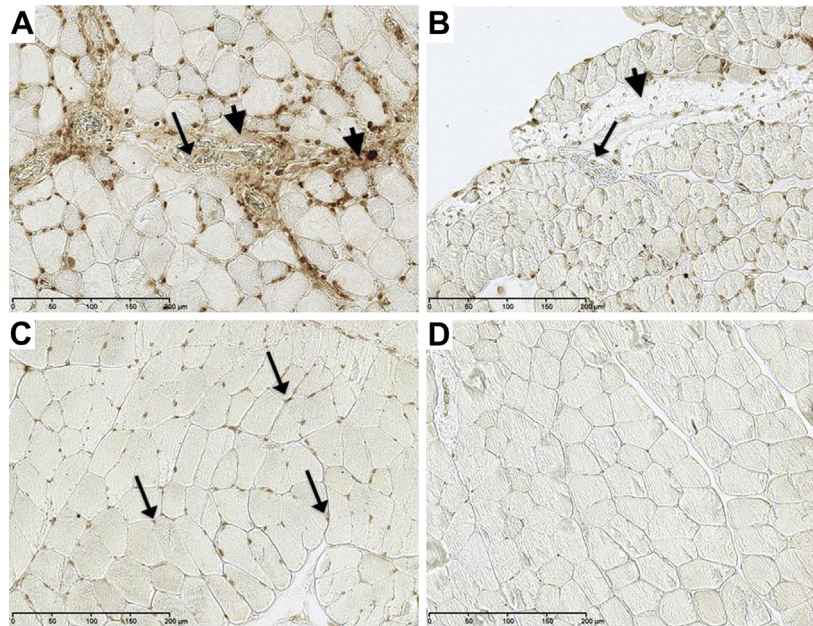


**Fig 3.** Representative images are shown for immunostaining for neutrophil extracellular traps (NETs) in murine hind limb ischemia-reperfusion (IR) injury using the monoclonal antihistone H2A/H2B/DNA complex antibody. **A**, Wild-type (WT) tissue sections show extensive immunostaining for NETs (*brown*) in interstitial tissue (*arrowhead*) and in thrombi (*arrow*) within vessels. There is increased cellular density in regions of intense NETs detection. **B**, Tissue section from Toll-like receptor-4 mutant (TLR4m) mice shows minimal if any interstitial (*arrowhead*) and intravascular NETs (*arrow*) immunostaining. **C**, Contralateral hind limb muscle fibers are normal, with positive immunostaining only in the nuclei of muscle fibers. **D**, Negative control. The *black bar* in each image represents 200  $\mu\text{m}$ .

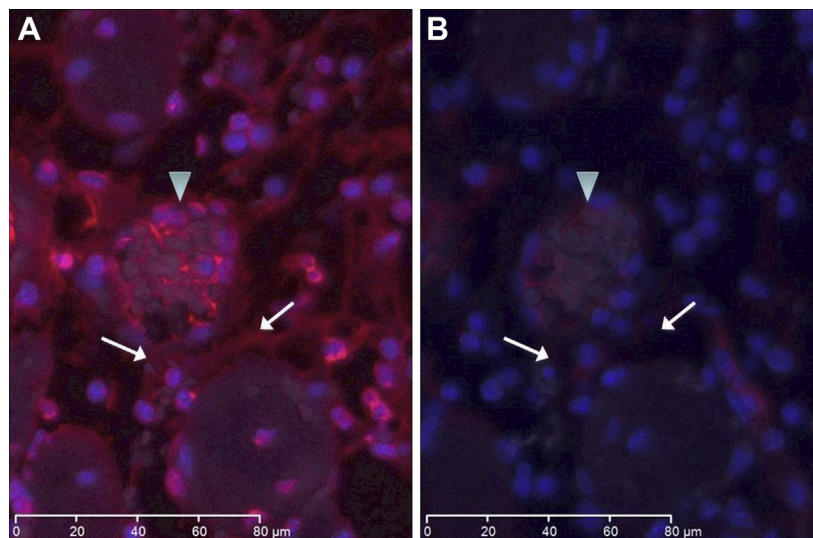


**Fig 4.** Immunofluorescent images show neutrophil extracellular traps (NETs) in *red* and nuclear DNA in *blue* in wild-type tissue section with and without DNase treatment. **A**, Wild-type (WT) tissue section demonstrates detection of NETs in a thrombosed vein (*arrowhead*) and in the interstitium (*arrows*). **B**, Adjacent tissue section was immunostained for NETs after an initial incubation with DNase enzyme. The section shows significant decrease in NET signal, suggesting that nuclease pretreatment markedly reduced the level of antigen available for detection. The *white bar* in each image represents 80  $\mu\text{m}$ .

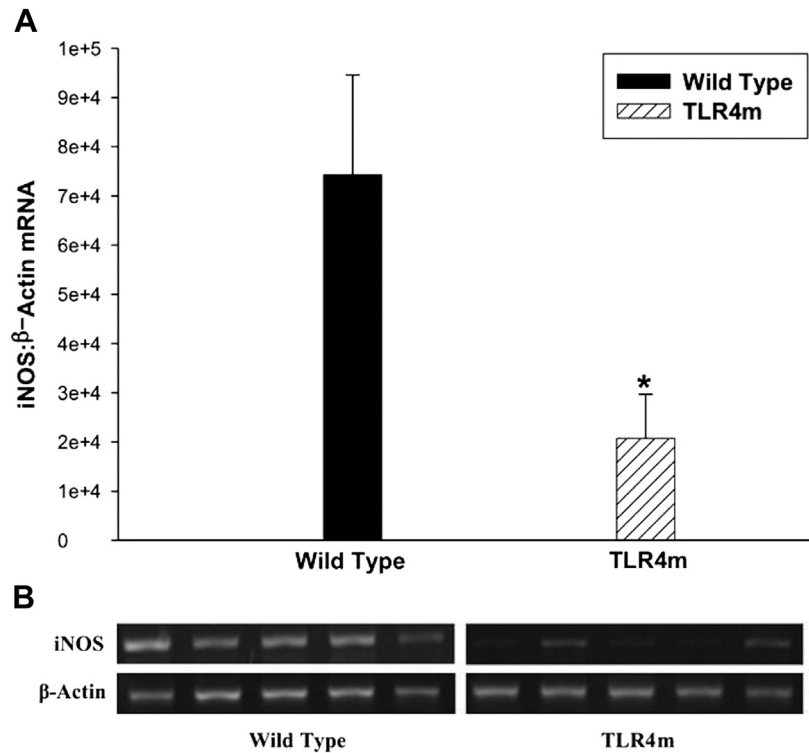


**Fig 5.** Inducible nitric oxide synthase (*iNOS*) messenger RNA (*mRNA*) expression is seen in ischemia-reperfusion (IR) injured murine skeletal muscles using semi-quantitative reverse-transcription polymerase chain reaction. **A**, Toll-like receptor-4 mutant (*TLR4m*) mice had significantly less *iNOS* mRNA expression than wild-type (WT) mice ( $*P < .03$ ) normalized to  $\beta$ -actin. **B**, A representative image of the agarose gel shows the *iNOS* and  $\beta$ -actin bands from the two groups of tissue samples.

samples. TLR4m serum samples showed decreased levels of the CXC cytokine KC compared with WT serum samples; however, this did not reach statistical difference ( $62 \pm 9$  vs  $88 \pm 32$  pg/mL, respectively;  $P = .08$ ; Fig 7, A). In contrast, serum MCP-1 levels in the TLR4m group were significantly lower than the WT group (TLR4,  $98 \pm 7$  vs WT,  $257 \pm 18$  pg/mL;  $n = 6$ ;  $P < .0002$ ; Fig 7, B). In addition, TLR4m mice had significantly higher levels of the proangiogenic factor VEGF (TLR,  $1272 \pm 377$  vs WT,  $54 \pm 4$  pg/mL;  $n = 6$ ;  $P < .015$ ; Fig 7, C). There were no detectable levels of KC, MCP-1, or VEGF in the serum of nonischemic WT and TLR4m mice. These data suggest that the WT group demonstrates a state of greater systemic inflammation than the TLR4m group. Moreover, the higher levels of VEGF detected in the TLR4m mice may result from the greater viable tissue remaining in the hind limb that is attempting to heal itself.

## DISCUSSION

These data are the first to implicate a role for TLR4 and NETs in skeletal muscle IR injury. To date, the TLR family of proteins has been shown to play a pivotal role in mediating venous thrombosis and IR injury in the heart and brain.<sup>1,4,21</sup> In the studies in this report, skeletal muscle fiber injury was significantly reduced in TLR4m mice compared with the WT mice (Fig 1). The decreased level of muscle

fiber injury in the TLR4m group suggests that the ensuing intense inflammation in the WT group likely plays a significant role in enhancing the level of tissue injury. It is unclear whether this increased injury is a direct result of NF- $\kappa$ B pathway activity, which is known to induce proinflammatory and proapoptotic genes<sup>22</sup> or is a secondary effect of the innate immune system resulting from leukocyte infiltration.

An analysis of the extent of inflammatory cell infiltration in reperfused skeletal muscle revealed that the decreased muscle fiber injury in the TLR4m group was associated with substantially less infiltration of MPO-positive inflammatory cells (Fig 2). This observation of decreased MPO-positive cell infiltration with decreased tissue injury is consistent with experiments geared toward neutrophil depletion in models of myocardial and small intestine IR.<sup>23,24</sup> TLR4m mice also had substantially less accumulation of NETs upon reperfusion. Although NETs have been previously associated with cystic fibrosis,<sup>25</sup> venous thrombosis,<sup>9</sup> bacterial sepsis,<sup>16</sup> and cell death,<sup>8</sup> this is the first demonstration that NETs are present in reperfused skeletal muscle. Because the accumulation of leukocytes in the injured muscle tissue corresponded to a marked detection of NETs, this strongly suggests that neutrophils are the most likely source of NETs in the injured muscle tissue; this is consistent with previous work demonstrating neutrophils as the dominant source



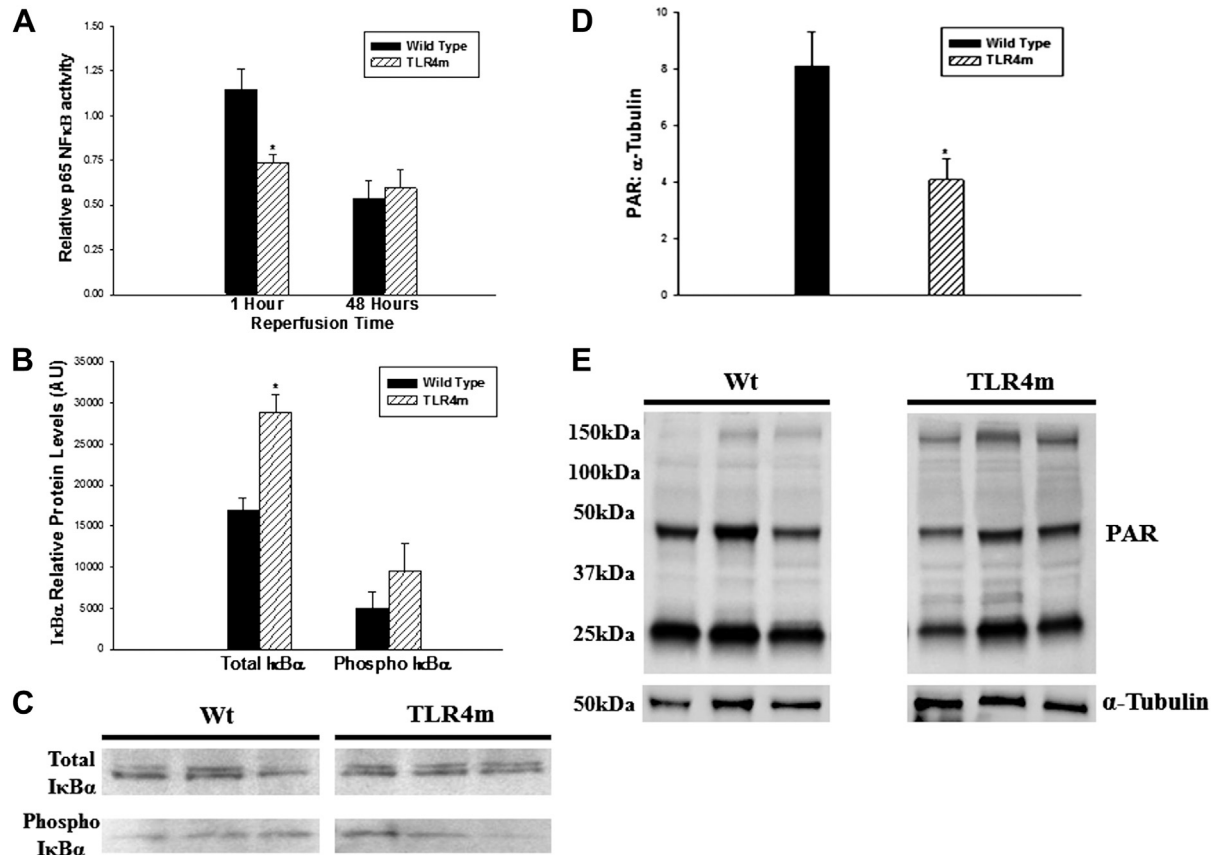


**Fig 6.** **A**, Relative detection of p65 nuclear factor (*NF*)- $\kappa$ B activity using an enzyme-linked immunosorbent assay is shown in murine hind limb muscle tissue after ischemia-reperfusion (IR). Toll-like receptor-4 mutant (*TLR4m*) mice had less p65 *NF*- $\kappa$ B activity than wild-type (*Wt*) mice after 1.5 hours of ischemia and 1 hour of reperfusion ( $*P = .0025$ ). By 48 hours there was no difference in p65 *NF*- $\kappa$ B activity detected between the two groups. **B**, Protein levels of the  $\alpha$ -subunit of inhibitor of *NF*- $\kappa$ B light polypeptide gene enhancer (*IκBα*) were quantitated using a Western blot analysis after 1.5 hours of ischemia and 1 hour of reperfusion. *TLR4m* mice had significantly greater levels of total *IκBα* in reperfused skeletal muscle than *Wt* mice ( $*P < .01$ ). In contrast, there was no significant difference in the Ser32-phosphorylation of *IκBα*. **C**, Representative Western blot analysis of three *Wt* and three *TLR4m*-derived muscle tissues. **D**, *TLR4m* mice showed significant decrease in the poly adenosine diphosphate ribose-modified (*PAR*) proteins at 48 hours' reperfusion compared with *Wt* ( $*P = .032$ ). **E**, Representative Western blot image of the detected poly ADP ribose-modified proteins in three *Wt* and three *TLR4m* skeletal muscle tissues.

of NET production.<sup>8,12,16,26</sup> NETs may further enhance the inflammatory response directly by acting on TLRs or by histone-mediated mechanisms. Extracellular histones have been shown to produce pathologic responses seen in sepsis, such as cellular infiltration, endothelial cell dysfunction, thrombosis, and organ failure. TLR2 and TLR4 proteins were recently shown to mediate the sepsis-like response seen in extracellular histones, and these histones were shown to activate platelets contributing to the development of microvascular thrombosis.<sup>12,27-29</sup>

To determine whether DNase treatment, which is currently marketed as Pulmozyme (Genentech Inc, South San Francisco, Calif) used to treat NETs associated with cystic fibrosis,<sup>30</sup> could destroy NETs in skeletal muscle, DNase was directly added to the surface of mounted slides of *WT* reperfused skeletal muscle. DNase completely depleted the NETs signal from detection in this ex vivo

technique. This finding will prompt future exploration of the potential effectiveness of DNase therapy in an in vivo model of hind limb IR.

The effects of the *TLR4m* on skeletal muscle IR were not limited to the inflammatory cells. *TLR4m* mice had increased preservation of skeletal muscle high-energy phosphate levels (Fig 1, D). This finding is also consistent with findings of ethyl pyruvate as a treatment for skeletal muscle IR.<sup>31</sup> *TLR4m* mice had markedly decreased levels of iNOS mRNA expression, which is also consistent with decreased activation of macrophages in other models of inflammation.<sup>32,33</sup> The decreased activation of the *NF*- $\kappa$ B pathway indicates that the TLR4 receptor MyD88-dependent pathway likely modulates the *NF*- $\kappa$ B pathway activity during reperfusion injury. As expected, the decrease in *NF*- $\kappa$ B expression was associated with increased *IκBα* expression, which suggests that the decrease



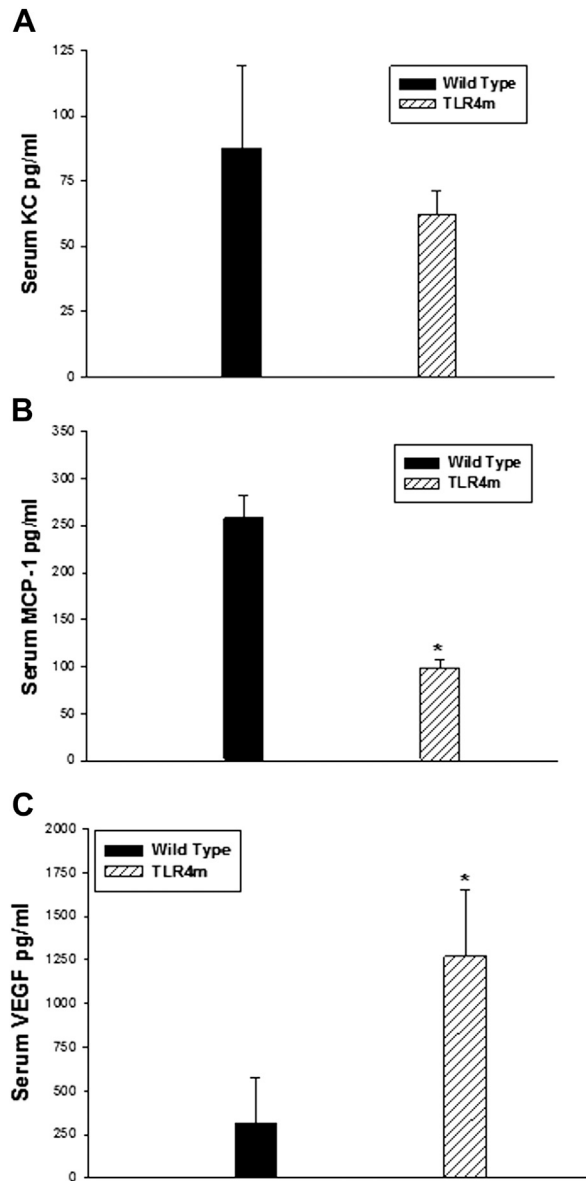


**Fig 7.** Quantitation of systemic markers of inflammation: (A) keratinocyte-derived cytokine (KC), (B) monocyte chemoattractant protein-1 (MCP-1), and (C) vascular endothelial growth factor (VEGF). **A**, Toll-like receptor-4 mutant (TLR4m) and wild-type (WT) mice had similar levels of the CXC cytokine KC. **B**, Serum MCP-1 levels in TLR4m mice, in contrast, were significantly lower than in WT mice after 48 hours of reperfusion (\* $P = .0002$ ). **C**, TLR4m mice also demonstrated a significantly higher level of the proangiogenic factor VEGF (\* $P = .015$ ).

in NF- $\kappa$ B is not a nonspecific event. Further evidence to suggest the specificity of decreased cellular stress in the TLR4m mice subjected to hind limb IR was the observed decrease in PARP activation. A previous report from our laboratory using pharmacologic interventions in a clinically relevant post hoc scenario showed only a transient decrease in PARP activity at 7 hours of reperfusion,<sup>34</sup>

whereas in this report, a significant decrease in PARP activity was observed even at 48 hours of reperfusion.

TLR4m mice had substantially decreased systemic levels of the proinflammatory cytokine, MCP-1, but not KC. MCP-1 deficiency has been shown to alter skeletal muscle healing,<sup>35</sup> and thus, it is not clear that its reduction in the TLR4m is beneficial. MCP-1, like interleukin-6, may possibly have proinflammatory and anti-inflammatory properties at different times in a physiologic process. In contrast to decreased MCP-1, circulating levels of VEGF were increased in the TLR4m group. This may mean that inhibiting the activity of TLR4 may potentiate postischemic angiogenic pathways.

Our study has several limitations. The use of pharmacologic inhibitors of TLR4 or its downstream intracellular signaling proteins would provide more information on the potential for clinically targeting TLR4.<sup>36-38</sup> Furthermore, it is not clear that the presence of NETs is deleterious or cytoprotective. This issue may be further studied by intravenous or intraperitoneal nuclease treatment, such as DNase-1, to degrade NETs. IR injury in MPO or nicotinamide adenine dinucleotide phosphate hydrogen oxidase knockout mice,<sup>39,40</sup> which are known to be deficient in the production of NETs, may also help demonstrate the potential role NETs may play in IR injury.

## CONCLUSIONS

We show that IR injury in the murine hind limb is modulated by a functional TLR4, suggesting that its inhibition before interventions in acute limb ischemia may be a potential strategy to minimize IR injury in patients. This increased muscle fiber injury is associated with marked infiltration of neutrophils and marked detection of NETs in the injured tissue. It is possible that NETs further intensify the hind limb muscle injury given the known deleterious effects of histones. Although ex vivo nuclease pretreatment of the hind limb muscle tissue sections diminishes the level of NET detection, it remains to be shown whether in vivo nuclease treatment will ameliorate IR injury in the hind limb muscle tissue.

## AUTHOR CONTRIBUTIONS

Conception and design: RO, HA, JJ, MW  
Analysis and interpretation: RO, HA, JJ, HY, MW  
Data collection: RO, HA, JJ, MW  
Writing the article: RO, HA, JJ, MW  
Critical revision of the article: RO, HA, JJ, MW  
Final approval of the article: RO, HA, JJ, MW  
Statistical analysis: HA, MW  
Obtained funding: MW  
Overall responsibility: MW  
RO and HA contributed equally to this article.

## REFERENCES

- Oyama J, Blais C Jr, Liu X, Pu M, Kobzik L, Kelly RA, et al. Reduced myocardial ischemia-reperfusion injury in toll-like receptor 4-deficient mice. *Circulation* 2004;109:784-9.

2. Shen XD, Gao F, Ke B, Zhai Y, Lassman CR, Tsuchihashi S, et al. Inflammatory responses in a new mouse model of prolonged hepatic cold ischemia followed by arterialized orthotopic liver transplantation. *Liver Transpl* 2005;11:1273-81.
3. Shen XD, Ke B, Zhai Y, Gao F, Busuttill RW, Cheng G, et al. Toll-like receptor and heme oxygenase-1 signaling in hepatic ischemia/reperfusion injury. *Am J Transplant* 2005;5:1793-800.
4. Tang SC, Arumugam TV, Xu X, Cheng A, Mughal MR, Jo DG, et al. Pivotal role for neuronal Toll-like receptors in ischemic brain injury and functional deficits. *Proc Natl Acad Sci U S A* 2007;104:13798-803.
5. Fan J, Kapus A, Marsden PA, Li YH, Oreopoulos G, Marshall JC, et al. Regulation of Toll-like receptor 4 expression in the lung following hemorrhagic shock and lipopolysaccharide. *J Immunol* 2002;168:5252-9.
6. Tsung A, Hoffman RA, Izuishi K, Critchlow ND, Nakao A, Chan MH, et al. Hepatic ischemia/reperfusion injury involves functional TLR4 signaling in nonparenchymal cells. *J Immunol* 2005;175:7661-8.
7. Wu H, Chen G, Wyburn KR, Yin J, Bertolino P, Eris JM, et al. TLR4 activation mediates kidney ischemia/reperfusion injury. *J Clin Invest* 2007;117:2847-59.
8. Fuchs TA, Abed U, Goosmann C, Hurwitz R, Schulze I, Wahn V, et al. Novel cell death program leads to neutrophil extracellular traps. *J Cell Biol* 2007;176:231-41.
9. Brill A, Fuchs TA, Savchenko AS, Thomas GM, Martinod K, De Meyer SF, et al. Neutrophil extracellular traps promote deep vein thrombosis in mice. *J Thromb Haemost* 2012;10:136-44.
10. Brinkmann V, Reichard U, Goosmann C, Fauler B, Uhlemann Y, Weiss DS, et al. Neutrophil extracellular traps kill bacteria. *Science* 2004;303:1532-5.
11. Oklu R, Albadawi H, Watkins MT, Monestier M, Sillesen M, Wicky S. Detection of extracellular genomic DNA scaffold in human thrombus: implications for the use of deoxyribonuclease enzymes in thrombolysis. *J Vasc Interv Radiol* 2012;23:712-8.
12. Clark SR, Ma AC, Tavener SA, McDonald B, Goodarzi Z, Kelly MM, et al. Platelet TLR4 activates neutrophil extracellular traps to ensnare bacteria in septic blood. *Nat Med* 2007;13:463-9.
13. Fuchs TA, Brill A, Duerschmied D, Schatzberg D, Monestier M, Myers DD Jr, et al. Extracellular DNA traps promote thrombosis. *Proc Natl Acad Sci U S A* 2010;107:15880-5.
14. Poltorak A, He X, Smirnova I, Liu MY, Van Huffel C, Du X, et al. Defective LPS signaling in C3H/HeJ and C57BL/10ScCr mice: mutations in Tlr4 gene. *Science* 1998;282:2085-8.
15. Crawford RS, Hashmi FF, Jones JE, Albadawi H, McCormack M, Eberlin K, et al. A novel model of acute murine hindlimb ischemia. *Am J Physiol Heart Circ Physiol* 2007;292:H830-7.
16. McCormack MC, Kwon E, Eberlin KR, Randolph M, Friend DS, Thomas AC, et al. Development of reproducible histologic injury severity scores: skeletal muscle reperfusion injury. *Surgery* 2008;143:126-33.
17. Doring Y, Soehnlein O, Drechsler M, Shagdarsuren E, Chaudhari SM, Meiler S, et al. Hematopoietic interferon regulatory factor 8-deficiency accelerates atherosclerosis in mice. *Arterioscler Thromb Vasc Biol* 2012;32:1613-23.
18. Schreiber A, Pham CT, Hu Y, Schneider W, Luft FC, Kettritz R. Neutrophil serine proteases promote IL-1beta generation and injury in necrotizing crescentic glomerulonephritis. *J Am Soc Nephrol* 2012;23:470-82.
19. Losman MJ, Fasy TM, Novick KE, Monestier M. Monoclonal autoantibodies to subnucleosomes from a MRL/Mp(-)/+ mouse. Oligoclonality of the antibody response and recognition of a determinant composed of histones H2A, H2B, and DNA. *J Immunol* 1992;148:1561-9.
20. Sappington PL, Cruz RJ Jr, Harada T, Yang R, Han Y, Englert JA, et al. The ethyl pyruvate analogues, diethyl oxalopropionate, 2-acetamidoacrylate, and methyl-2-acetamidoacrylate, exhibit anti-inflammatory properties in vivo and/or in vitro. *Biochem Pharmacol* 2005;70:1579-92.
21. Henke PK, Mitsuya M, Luke CE, Elfline MA, Baldwin JF, Detrick KB, et al. Toll-like receptor 9 signaling is critical for early experimental deep vein thrombosis resolution. *Arterioscler Thromb Vasc Biol* 2011;31:43-9.
22. Akira S, Takeda K. Toll-like receptor signalling. *Nat Rev Immunol* 2004;4:499-511.
23. Granfeldt A, Jiang R, Wang NP, Mykytenko J, Eldaif S, Deneve J, et al. Neutrophil inhibition contributes to cardioprotection by post-conditioning. *Acta Anaesthesiol Scand* 2012;56:48-56.
24. Liu Y, Kalogeris T, Wang M, Zuidema MY, Wang Q, Dai H, et al. Hydrogen sulfide preconditioning or neutrophil depletion attenuates ischemia-reperfusion-induced mitochondrial dysfunction in rat small intestine. *Am J Physiol Gastrointest Liver Physiol* 2012;302:G44-54.
25. Marcos V, Zhou Z, Yildirim AO, Bohla A, Hector A, Vitkov L, et al. CXCR2 mediates NADPH oxidase-independent neutrophil extracellular trap formation in cystic fibrosis airway inflammation. *Nat Med* 2010;16:1018-23.
26. Wang Y, Li M, Stadler S, Correll S, Li P, Wang D, et al. Histone hypercitrullination mediates chromatin decondensation and neutrophil extracellular trap formation. *J Cell Biol* 2009;184:205-13.
27. Massberg S, Grahl L, von Bruchl ML, Manukyan D, Pfeiler S, Goosmann C, et al. Reciprocal coupling of coagulation and innate immunity via neutrophil serine proteases. *Nat Med* 2010;16:887-96.
28. Xu J, Zhang X, Monestier M, Esmon NL, Esmon CT. Extracellular histones are mediators of death through TLR2 and TLR4 in mouse fatal liver injury. *J Immunol* 2011;187:2626-31.
29. Xu J, Zhang X, Pelayo R, Monestier M, Ammolto CT, Semeraro F, et al. Extracellular histones are major mediators of death in sepsis. *Nat Med* 2009;15:1318-21.
30. Dubois AV, Gauthier A, Brea D, Varaigne F, Diot P, Gauthier F, et al. Influence of DNA on the activities and inhibition of neutrophil serine proteases in cystic fibrosis sputum. *Am J Respir Cell Mol Biol* 2012;47:80-6.
31. Crawford RS, Albadawi H, Atkins MD, Jones JJ, Conrad MF, Austen WG Jr, et al. Posts ischemic treatment with ethyl pyruvate prevents adenosine triphosphate depletion, ameliorates inflammation, and decreases thrombosis in a murine model of hind-limb ischemia and reperfusion. *J Trauma* 2011;70:103-10.
32. Muthupalani S, Ge Z, Feng Y, Rickman B, Mobley M, McCabe A, et al. Systemic macrophage depletion inhibits *Helicobacter bilis*-induced proinflammatory cytokine-mediated typhlocolitis and impairs bacterial colonization dynamics in a BALB/c Rag2<sup>-/-</sup> mouse model of inflammatory bowel disease. *Infect Immun* 2012;80:4388-97.
33. Riquelme P, Tomiuk S, Kammler A, Fandrich F, Schlitt HJ, Geissler EK, et al. IFN-gamma-induced iNOS expression in mouse regulatory macrophages prolongs allograft survival in fully immunocompetent recipients. *Mol Ther* 2013;21:409-22.
34. Crawford RS, Albadawi H, Atkins MD, Jones JE, Yoo HJ, Conrad MF, et al. Posts ischemic poly (ADP-ribose) polymerase (PARP) inhibition reduces ischemia reperfusion injury in a hind-limb ischemia model. *Surgery* 2010;148:110-8.
35. Abbruzzese TA, Albadawi H, Kang J, Patel VI, Yoo JH, Lamuraglia GM, et al. Enoxaparin does not ameliorate limb ischemia-reperfusion injury. *J Surg Res* 2008;147:260-6.
36. Mullarkey M, Rose JR, Bristol J, Kawata T, Kimura A, Kobayashi S, et al. Inhibition of endotoxin response by e5564, a novel Toll-like receptor 4-directed endotoxin antagonist. *J Pharmacol Exp Ther* 2003;304:1093-102.
37. Parker LC, Whyte MK, Vogel SN, Dower SK, Sabroe I. Toll-like receptor (TLR)2 and TLR4 agonists regulate CCR expression in human monocytic cells. *J Immunol* 2004;172:4977-86.
38. Wu Y, Lousberg EL, Moldenhauer LM, Hayball JD, Collier JK, Rice KC, et al. Inhibiting the TLR4-MyD88 signalling cascade by genetic or pharmacological strategies reduces acute alcohol-induced sedation and motor impairment in mice. *Br J Pharmacol* 2012;165:1319-29.
39. Gao XP, Standiford TJ, Rahman A, Newstead M, Holland SM, Dinauer MC, et al. Role of NADPH oxidase in the mechanism of lung neutrophil sequestration and microvessel injury induced by Gram-negative sepsis: studies in p47phox<sup>-/-</sup> and gp91phox<sup>-/-</sup> mice. *J Immunol* 2002;168:3974-82.
40. Nguyen HX, Lusic AJ, Tidball JG. Null mutation of myeloperoxidase in mice prevents mechanical activation of neutrophil lysis of muscle cell membranes in vitro and in vivo. *J Physiol* 2005;565:403-13.